The Crystal Structure of *Sulfolobus solfataricus* Elongation Factor 1α in Complex with Magnesium and GDP[†,‡]

Luigi Vitagliano,[&,§] Alessia Ruggiero,[||] Mariorosario Masullo,[⊥,#] Piergiuseppe Cantiello,[#] Paolo Arcari,[#,%] and Adriana Zagari[*,&,||,%]

Istituto di Biostrutture e Bioimmagini, CNR, via Mezzocannone 6, I-80134 Napoli, Italy, Centro interuniversitario di ricerca sui Peptidi bioattivi (CIRPEB), via Mezzocannone 6, I-80134 Napoli, Italy, Dipartimento di Chimica Biologica, Sezione di Biostrutture, Università degli Studi di Napoli Federico II, via Mezzocannone 6, I-80134 Napoli, Italy, Dipartimento di Scienze Farmacobiologiche, Università degli Studi di Catanzaro "Magna Graecia", Roccelletta di Borgia 88021 Catanzaro, Italy, Dipartimento di Biochimica e Biotecnologie Mediche, Università degli Studi di Napoli Federico II, Via Pansini 5, I-80131 Napoli, Italy, CEINGE, Biotecnologie Avanzate Scarl, Via Comunale Margherita 482, I-80145 Napoli, Italy

Received December 30, 2003; Revised Manuscript Received March 10, 2004

ABSTRACT: Recent studies have shown that elongation factors extracted from archaea/eukarya and from eubacteria exhibit different structural and functional properties. Along this line, it has been demonstrated that, in contrast to EF-Tu, *Sulfolobus solfataricus* EF-1α in complex with GDP (*Ss*EF-1α·GDP) does not bind Mg^{2+}, when the ion is present in the crystallization medium at moderate concentration (5 mM). To further investigate the role that magnesium plays in the exchange process of EF-1α and to check the ability of *Ss*EF-1α·GDP to bind the ion, we have determined the crystal structure of *Ss*EF-1α·GDP in the presence of a nonphysiological concentration (100 mM) of Mg^{2+}. The analysis of the coordination of Mg^{2+} unveils the structural bases for the marginal role played by the ion in the nucleotide exchange process. Furthermore, nucleotide exchange experiments carried out on a truncated form of *Ss*EF-1α, consisting only of the nucleotide binding domain, demonstrate that the low affinity of *Ss*EF-1α·GDP for Mg^{2+} is due to the local architecture of the active site and does not depend on the presence of the other two domains. Finally, considering the available structures of EF-1α, a detailed mechanism for the nucleotide exchange process has been traced. Notably, this mechanism involves residues such as His14, Arg95, Gln131, and Glu134, which are strictly conserved in all archaea and eukarya EF-1α sequences hitherto reported.

Guanine nucleotide binding proteins (GNBP)[1] are enzymes involved in fundamental biological processes (*1*, *2*). The members of this family play crucial roles in cell growth and proliferation, signal transduction, membrane trafficking, and protein biosynthesis. In these enzymes, the transition from the active GTP-bound form to the inactive GDP-bound state is associated with a conformational switch, which activates important cellular processes. Although the magnitude of the conformational change varies among different GNBP, it represents a fundamental step for their function.

In GNBP involved in protein biosynthesis, the conformational changes associated with the GTP hydrolysis produces a major rearrangement of the multidomain structure of these enzymes. The most studied translation GNBP are the elongation factors that transport the aminoacyl-tRNA to the ribosome (EF-Tu in bacteria and EF-1α in eukarya and archaea) (*3*−*5*). In carrying out their biological functions, these enzymes interact with several cellular components: GTP, GDP, aminoacyl-tRNA, ribosome, and the exchange factors (EF-Ts in eubacteria and EF-1β in eukarya and archaea), which activate these GNBP by favoring the release of the GDP. In the past decade, a number of impressive three-dimensional (3D) structure determinations of EF-Tu have shed light on the structural details of the elongation cycle in eubacteria. These investigations have provided a clear picture of the conformational flexibility of EF-Tu, whose shape is modulated by the interactions with GDP (*6*−*9*), GDPNP (*10*, *11*), aminoacyl-tRNA (*12*−*14*), EF-Ts (*15*, *16*), and antibiotics (*17*, *18*).

On the other hand, there is limited structural information available on the translation elongation factors isolated from eukarya and archaea. Only recently, the 3D structures of the

[†] This work was financially supported by PRIN 2003 (Rome).

[‡] The atomic parameters (code 1skq) have been deposited in the Protein Data Bank.

* To whom correspondence should be addressed. Telephone: +39-0812536614. Fax: +39-0812536603. E-mail: zagari@chemistry.unina.it.

[&] Istituto di Biostrutture e Bioimmagini, CNR.

[§] CIRPEB.

[||] Dipartimento di Chimica Biologica, Università degli Studi di Napoli Federico II.

[⊥] Università degli Studi di Catanzaro "Magna Graecia".

[#] Dipartimento di Biochimica e Biotecnologie Mediche, Università degli Studi di Napoli Federico II.

[%] CEINGE, Biotecnologie Avanzate Scarl.

[1] Abbreviations: GNBP, guanine nucleotide binding proteins; EF-Tu·GDP, complex of the elongation factor Tu with GDP; *Ss*EF-1α·GDP, complex of *Sulfolobus solfataricus* EF-1α with GDP; *Ss*EF-1α·GDP/Mg^{2+}, complex of *S. solfataricus* EF-1α with GDP and Mg^{2+}; *Sc*EF-1β/EF-1α complex of *Saccharomyces cerevisiae* EF-1α with the exchange factor EF-1β; *Sc*EF-1β/EF-1α·GDP, complex of *S. cerevisiae* EF-1α with EF-1β and GDP; *Ss*(G)EF-1α, guanine nucleotide binding domain of *S. solfataricus* EF-1α; ppGpp, guanosine-5′-diphosphate-3′-diphosphate.

10.1021/bi0363331 CCC: $27.50
Published on Web 05/04/2004

complex of EF-1α with the catalytic C-terminal domain of EF-1*β* from *Saccharomyces cerevisiae* (*Sc*EF-1*β*/EF-1α·GDP) (*19*), and the structure of EF-1α from the archaeon *Sulfolobus solfataricus* in complex with GDP (*Ss*EF-1α·GDP) have been determined (*20*). The structure of the complex *Sc*EF-1α/EF-1*β* has revealed that in eukarya the association between elongation and exchange factors is completely different from that observed in eubacteria (*19*). Taking into account the structures of the complex *Sc*EF-1*β*/EF-1α bound to GDP or GDPNP (*21*) and the structure of EF-Tu·GDP, a mechanism for the nucleotide exchange process in EF-1α has been proposed, based on the disruption of the magnesium binding site.

Surprisingly, the structure of *Ss*EF-1α·GDP complex showed that, in contrast to EF-Tu and most of the other GTPases, the interactions between the protein and the nucleotide are not mediated by magnesium, despite the presence of the ion (5 mM) in the crystallization medium (*20*). Complementary biochemical studies have supported the crystallographic results, by showing that the addition of Mg^{2+}, although essential to the GTPase activity, has only a marginal effect on the nucleotide exchange process (*20*). Therefore, these findings undermined the previously proposed (*21*) exchange mechanism in EF-1α.

To further investigate the role the magnesium plays in the GDP binding to EF-1αs and particularly to check the ability of *Ss*EF-1α·GDP to bind this ion, we have determined the crystal structure of the *Ss*EF-1α·GDP in the presence of a nonphysiological concentration (100 mM) of Mg^{2+}. In addition, nucleotide exchange experiments have been carried out on a truncated form of SsEF-1α to unveil whether the low affinity for Mg^{2+} depends on the local architecture of the active site or on the domain organization of the enzyme. Finally, comparing the structures of *Ss*EF-1α·GDP/Mg^{2+}, *Ss*EF-1α·GDP, *Sc*EF-1*β*/EF-1α·GDP, and *Sc*EF-1*β*/EF-1α a detailed mechanism for the nucleotide exchange process of EF-1α has been proposed.

EXPERIMENTAL PROCEDURES

Preparation of SsEF-1α. The expression vector used was a pT7-7 derivative, containing the gene encoding the elongation factor 1α from *S. solfataricus* (*22*). The recombinant plasmid was transferred into the *Escherichia coli* BL21 (DE3) strain. The transformed cells were grown overnight at 37 °C in 10 mL of L-broth containing 100 *μ*g/mL ampicillin. The culture was then diluted 1:100 to a final volume of 1 L and grown up to an absorbance of 0.8 at 600 nm; induction (3 h) was performed by adding isopropyl-*β*-D-thiogalactopyranoside up to a final concentration of 0.4 mM. The bacterial cells were collected by centrifugation, resuspended in a buffer (6 mL/g of wet cells) containing 20 mM Tris/HCl (pH 7.8), 50 mM KCl, 10 mM $MgCl_2$, and 15% (v/v) glycerol and 1 mM phenylmethanesulfonylfluoride, and disrupted by a constant system of cell disruption at 2 kbar (Constant System, Ltd, U.K.). The recombinant protein was purified following the procedure previously reported (*22*). The protein was stored at −20 °C in a buffer containing 20 mM Tris/HCl (pH 7.8), 50 mM KCl, 10 mM $MgCl_2$, and 50% (v/v) glycerol.

Crystallization, Crystal Data and Refinement of SsEF-1α·GDP/Mg^{2+}. As for the complex *Ss*EF-1α·GDP (*23*), crystals of *Ss*EF-1α·GDP/Mg^{2+} were grown using PEG 4000 and propan-2-ol as precipitants. Diffraction quality crystals were obtained using the microbatch under oil technique at 4 °C and a protein concentration of 6 mg/mL. The final concentration of the components of the crystallization medium was 8% (w/v) PEG8000, 8% (v/v) propan-2-ol, 4 mM Na citrate (pH 5.6), and 100 mM $MgCl_2$.

Table 1: Data Collection and Refinement Statistics

Crystal Data	
a (Å)	61.95
b (Å)	113.83
c (Å)	81.08
β (°)	90.1
space group	$P2_1$
Data Processing	
resolution range (Å)	30−1.80
no. of observations	301602
no. of unique reflections	98914
$\langle I/\sigma(i)\rangle$	24.6 (2.3)[a]
completeness (%)	94.3 (80.7)[a]
R-merge[b] (%)	3.5 (34.3)[a]
Refinement	
resolution range (Å)	30−1.80
R-factor[c]	0.219
R-free[d]	0.255
no. protein atoms	6506
no. of GDP molecules	2
no. of magnesium ions	1
no. of water molecules	353
Root-Mean-Square Deviations from Ideal Values	
bond lengths (Å)	0.019
bond angles (°)	2.0
dihedral angles (°)	25.5
improper angles (°)	1.3

[a] The values given in parentheses refer to the highest resolution shell (1.86−1.80 Å). [b] $R\text{-merge} = \sum_{hkl}\sum_i|I_i - \langle I\rangle|/|I_i|$. [c] $R\text{-factor} = \sum_{hkl}(||F_{hkl\text{obs}}| - k|F_{hkl\text{calc}}||)/\sum_{hkl}|F_{hkl\text{obs}}|$. [d] $R\text{-free} = \sum_{\boldsymbol{h}}(||F_{\text{obs}}| - k|F_{\text{calc}}||)/\sum_{\boldsymbol{h}}|F_{\text{obs}}|$ where $\boldsymbol{h}$ is a statistical subset (9.3%) of data.

Data collection was performed at ESRF synchrotron beam line ID-14-1 (Grenoble, France) at 100 K. The crystals were frozen after a 1-min soak in a solution containing 10% (w/v) PEG8000, 10% (v/v) propan-2-ol, 4 mM sodium citrate (pH 5.6), 100 mM $MgCl_2$, and 20% (v/v) ethylenglycol as cryoprotectant. Diffraction data were registered up to 1.8 Å resolution. The crystals of *Ss*EF-1α·GDP/Mg^{2+} are isomorphous to those of *Ss*EF-1α·GDP and contain two independent protein molecules in the asymmetric unit. Diffraction data were processed using the HKL package (*24*). A summary of the statistics of the data collection is reported in Table 1.

The structure of *Ss*EF-1α·GDP/Mg^{2+} was refined using the structure of *Ss*EF-1α·GDP (Protein Data Bank code 1JNY) (*20*) as a starting model. The crystallographic refinements were alternated by manual modifications of the model carried out with the program O (*25*). The rigid body refinement of the initial model, which included neither water molecules nor GDP, converged to an *R*-factor of 0.330 (*R*-free 0.329) using diffraction data in the resolution range 6.0−1.85 Å. Since the early stages of the refinement, it was clear that an electron density peak compatible with a Mg^{2+} ion was present in the active site of the molecule of the asymmetric unit designated as molecule A (Figure 1A), which is characterized by a better defined electron density and lower B factors. The inspection of the active site cleft of molecule B reveals that no ion is bound to the GDP of

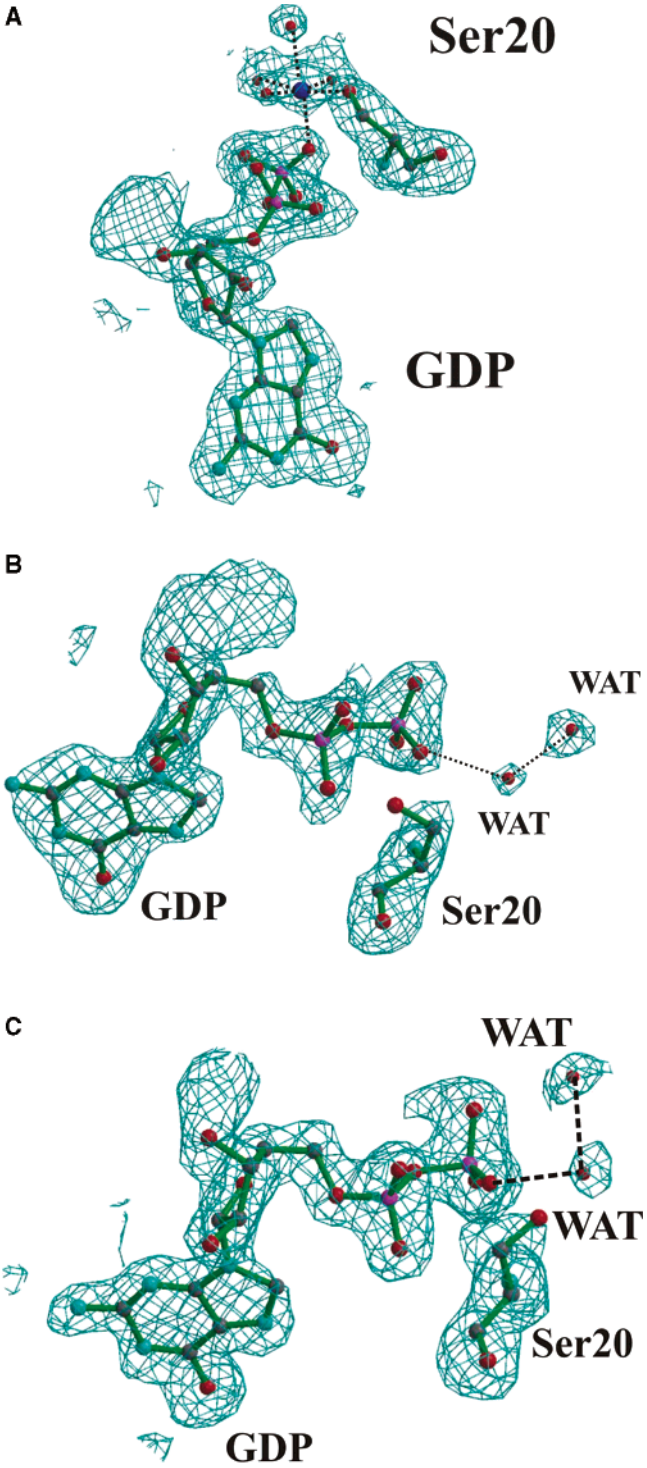

FIGURE 1: Omit $F_o - F_c$ electron density maps corresponding to the active sites of molecule A (A) and molecule B (B) of the asymmetric unit. The magnesium ion is colored in blue. A large electron density peak, located in proximity of the O3′ atom of the ribose, is evident in both molecules (see the text for details). In panel C is reported the omit $F_o - F_c$ electron density map corresponding to the active site region of the recombinant wild-type *Ss*EF-1α·GDP. This structure has been refined to an *R*-factor value of 22.8 (*R*-free 26.1) using diffraction data in the resolution range 20−1.85 Å.

this protein molecule (Figure 1B). Similar to what was observed in the EF-1α·GDP structure derived from crystals grown in 5 mM $MgCl_2$ (*20*), the phosphate groups of GDP molecule bound to molecule B are surrounded only by water molecules.

In both molecules, a second peak was located in proximity of the O3′ oxygen of the sugar moiety of the GDP (Figure 1A,B). This extra electron density likely corresponds to a phosphate group of the GDP analogue guanosine-5′-diphosphate-3′-diphosphate (ppGpp) (see below for details).

In the final stage of the refinement, water molecules were identified by evaluating the shape of the electron density and the distance of potential hydrogen bond donors and/or acceptors. The final model, which includes 353 water molecules, was refined to an *R*-factor of 0.219 (*R*-free 0.255) in the resolution range 30.0−1.80 Å. This model presents a good stereochemistry (Table 1).

The figures were drawn using the programs O (*25*), Molscript (*26*), Bobscript (*27*), and Raster3D (*28*).

Chemical Nature of the Nucleotide Bound to SsEF-1α. To identify the chemical nature of the nucleotide bound to the active site of the enzyme, chromatography and mass spectrometry experiments were carried out. The nucleotide was separated from the protein by HPLC chromatography in denaturing conditions. In particular, the nucleotide was isolated using a reverse phase C18 column under ion-pairing conditions. The isocratic elution was conducted using a buffer containing 50 mM potassium phosphate (pH 6.7), 10 mM tetrabutylammonium hydrogensulfate, and 10% (v/v) acetonitrile. The molecular weight of the nucleotide was determined by MALDI-TOF mass spectrometry. A clear peak at 625.60 *m*/*z* was interpreted as due to ppGpp (molecular mass 602.12 Da) complexed with a sodium ion (molecular mass 22.99 Da).

Preparation and Nucleotide Exchange of SsEF-1α Guanine Nucleotide Binding Domain. The truncated form of *Ss*EF-1α corresponding to the guanine nucleotide binding domain of the enzyme (*Ss*(G)EF-1α) was prepared by introducing a stop codon after the triplet encoding Ile 235 as previously reported (*29*). *Ss*(G)EF-1α·[^{3}H]GDP was prepared by incubating 2 μM *Ss*(G)EF-1α with 20 μM [^{3}H]-GDP (specific activity 520 cpm/pmol) for 30 min at 60 °C. The nucleotide exchange activity was measured at 60 °C in a reaction mixture containing 1 μM *Ss*(G)EF-1α·[^{3}H]GDP in 350 μL of 20 mM Tris·HCl buffer (pH 7.8) and 50 mM KCl. The effect of Mg^{2+} was evaluated in the presence of either 10 mM $MgCl_2$ or 10 mM EDTA. The exchange reaction was started by the addition of either GDP or GTP at 1 mM final concentration.

RESULTS AND DISCUSSION

Overall Structure of SsEF-1α·GDP/Mg^{2+}. The structure of the complex *Ss*EF-1α·GDP/Mg^{2+} was derived from crystals grown in a medium containing 100 mM $MgCl_2$. The structure was refined to an *R*-factor of 0.219 (*R*-free 0.255) using diffraction data extending to 1.8 Å resolution. As for the complex, *Ss*EF-1α·GDP, the electron density is well defined for most of the protein residues. Disordered regions, not included in the final model, correspond to the fragments 1−3, 65−77, and 430−435 of both molecules present in the asymmetric unit. The overall structure of the enzyme is practically identical to the structure of *Ss*EF-1α·GDP, since the root-mean-square deviation on C^α atoms is as low as 0.27 Å. Therefore, the *Ss*EF-1α·GDP/Mg^{2+} complex preserves the domain organization of *Ss*EF-1α·GDP (Figure 2). The first domain (residues 4−235), which contains the

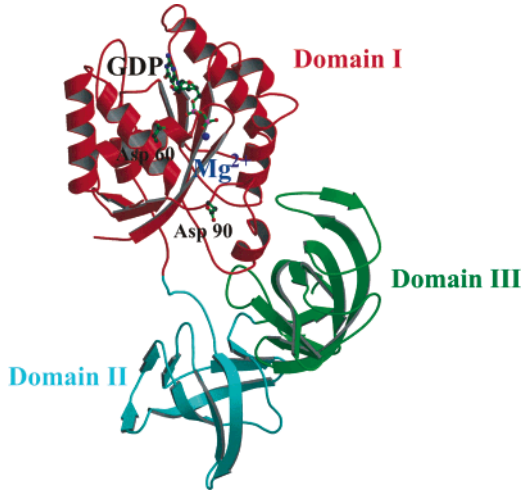

FIGURE 2: Overall structure of *Ss*EF-1α in complex with GDP and Mg^{2+}. The three domains are colored differently. The GDP, Asp60, Asp90, and Mg^{2+} (in blue) are also shown in ball-and-stick.

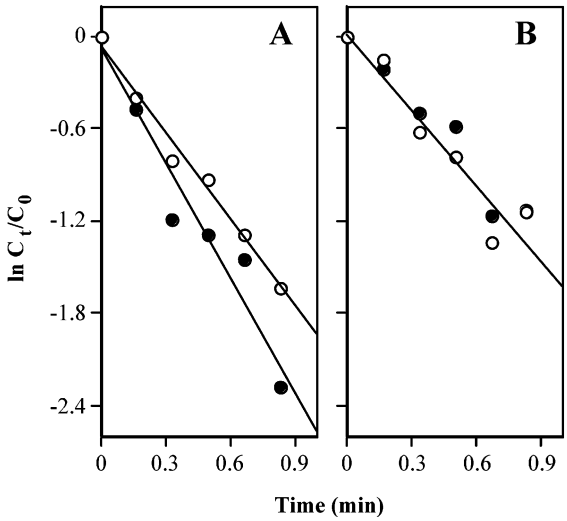

FIGURE 3: Nucleotide exchange on the isolated guanine nucleotide binding domain of *Ss*EF-1α: [^{3}H]GDP/GDP (A) and [^{3}H]GDP/GTP (B) exchange reactions in the presence of either 10 mM $MgCl_2$ (open circles) or 10 mM EDTA (filled circles). C_0 and C_t represent the initial concentration and the concentration at time *t* of *Ss*EF-1α·[^{3}H]GDP, respectively.

nucleotide binding site presents an α/β structure, whereas the other two domains (residues 236−335 and 336−430) display β-barrel structures.

The GDP Binding Site. The difference Fourier map in the active site region of the two molecules in the asymmetric unit clearly shows the presence of electron densities corresponding to the GDP molecules. However, a deeper investigation revealed the presence of extra peaks in these regions. In one molecule, designated as molecule A and characterized by a better defined electron density and lower B factors, two extra peaks were identified (Figure 1A). The first one was located in proximity of the β-phosphate of the GDP in the position typically occupied by the magnesium ion in EF-Tu structures. The presence of six ligands (four water molecules, an oxygen atom of the β-phosphate of the GDP, and the O^{γ} atom of Ser20), arranged in an octahedral coordination, provided unambiguous evidence for the presence of Mg^{2+} in the structure (Figure 1A). The second peak (8.0 and 5.5 sigma level in molecule A and B, respectively) was located in proximity of the O3′ oxygen of the sugar moiety of the GDP. The occurrence of this peak is not related to the presence of the magnesium in the crystallization medium since it has also been found in structure of the recombinant wild-type *Ss*EF-1α in complex with GDP derived from crystals grown in the absence of Mg^{2+} (Figure 1C). In addition, this peak has also been observed in the structure of a *Ss*EF-1α mutant complexed with GDP, whose crystals were also grown without Mg^{2+} (unpublished results). Notably, this electron density peak was not present in the previous structure of *Ss*EF-1α·GDP which was derived from a protein sample purified from *S. solfataricus* cells (Figure 2 of ref *20*). Therefore, the extra electron density may be due to some modifications of the nucleotide occurring upon protein expression and purification. It has been reported that, under particular conditions, bacteria produce a large amount of ppGpp and that ppGpp can bind to GNBP (*30*, *31*). Therefore, the electron density peak located in proximity of the O3′ oxygen could be ascribed to one of the two phosphates of the pyrophosphate moiety bound to the ribose. The second phosphate is likely to be disordered since it is exposed to the solvent. Although this hypothesis is supported by the mass spectrometry experiments reported in Experimental Procedures, the extra-phosphate moiety has not been modeled in the electron density.

A different picture emerges from the analysis of the electron density of the GDP binding pocket of molecule B (Figure 1B). In this case, only the extra electron density located nearby the O3′ oxygen atom of the ribose could be identified. On the other hand, there is no evidence of the electron density corresponding to the magnesium ion. Indeed, only water molecules surround the beta phosphate on analogy with the EF-1α structure derived from crystals grown in the presence of a limited amount of $MgCl_2$.

These findings indicate that the interactions between the *Ss*EF-1α·GDP and the magnesium are extremely weak because (i) a nonphysiological concentration of the ion is necessary to detect the binding, and (ii) only molecule A of the asymmetric unit binds the magnesium. The analysis of the coordination sphere of the Mg^{2+} bound to molecule A provides some clues about the weak affinity of *Ss*EF-1α·GDP for this ion. As shown in Figure 1A, Mg^{2+} is coordinated by one oxygen atom of the β-phosphate moiety of GDP, by the O^{γ} atom of Ser 20, and by four water molecules. Interestingly, in contrast to that generally observed for other GTPases bound to GDP and Mg^{2+}, these coordination water molecules are not involved in hydrogen bonding interactions with other residues of the protein. The side chains of the conserved residues Asp60 and Asp90, which are usually hydrogen bonded to the water molecules coordinating the Mg^{2+} in EF-Tu structures (*6*, *7*, *32*), are, in fact, very far from the ion (Figure 2). These missing interactions may account for the weak affinity of *Ss*EF-1α·GDP for Mg^{2+}.

It is worth mentioning that the binding of Mg^{2+} does not produce significant modifications on the structure of *Ss*EF-1α·GDP as shown by the very low root-mean-square deviation (0.27 Å) between *Ss*EF-1α·GDP and *Ss*EF-1α·GDP/Mg^{2+}. The only clear variation involves the side chain of Ser20 of molecule A, whose conformation was ambiguous in the structure of *Ss*EF-1α·GDP (*20*). Indeed, the interaction with the Mg^{2+} makes the electron density corresponding to

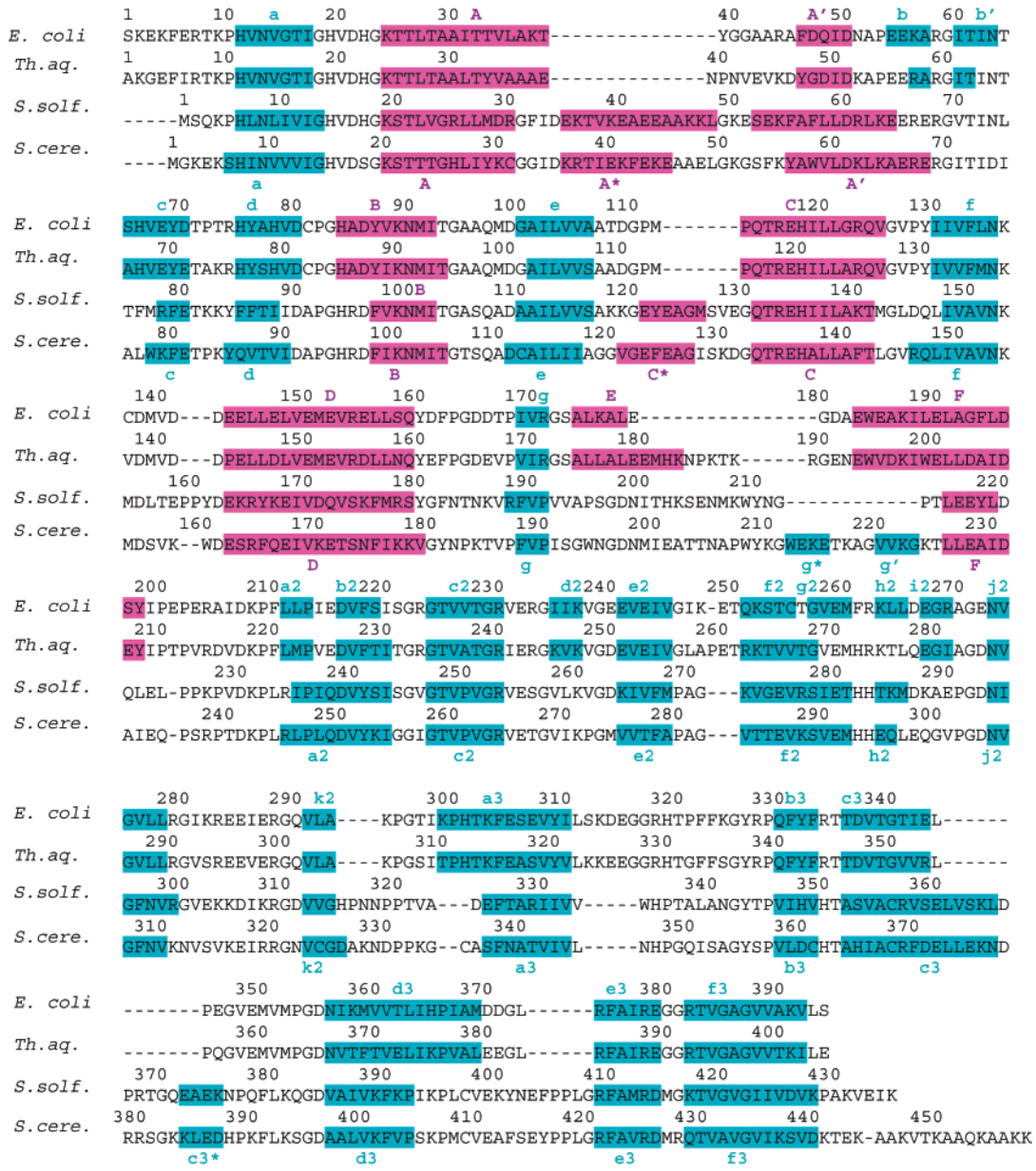

FIGURE 4: Sequence alignments of EF-Tu (*E. coli* and *Thermus aquaticus*) and EF-1α (*S. cerevisiae* and *S. solfataricus*) for which structural data have been reported. *β*-strand and α-helix regions are cyan and pink, respectively. The notation of the secondary structure elements of EF-Tu, reported in the first line, has been taken from Song et al. (*32*). A similar notation has been used for EF-1α (last line).

the side chain of this residue very well defined in *Ss*EF-1α·GDP/Mg^{2+}. Consistently, the side chain of molecule B Ser 20 remains somewhat disordered. The binding of Mg^{2+} does not have any effect on the region 65−77, which remains disordered as in *Ss*EF-1α·GDP (*20*).

Role of Magnesium on the Nucleotide Exchange Process of Ss(G)EF-1α. To identify the structural determinants of the low affinity of *Ss*EF-1α for Mg^{2+}, nucleotide exchange experiments were carried out on a truncated form (residues 1−235) of *Ss*EF-1α constituted only of the guanine nucleotide binding domain. This investigation was aimed at elucidating whether the reduced affinity for the magnesium is an intrinsic property of the GTPase domain or it can be due to the influence of the other domains. The latter hypothesis is apparently supported by the observation that the contacts between helix B (residues 97−102), which is directly linked to Asp90, and domain III represent the only relevant interdomain interactions in *Ss*EF-1α·GDP. In this scenario, the interactions between helix B and domain III may impede the participation of Asp90 to the binding of water molecules that coordinate the ion and therefore reduce the affinity of the protein for magnesium. It is also worth noting that the interactions of helix B with domain III are completely different in GDP complexes of EF-Tu and EF-1α.

The analysis of [^{3}H]GDP/GDP and [^{3}H]GDP/GTP exchange processes of *Ss*(G)EF-1α reveals that the magnesium ion at a concentration of 10 mM has minimal effects (Figure 3) as observed for the full-length *Ss*EF-1α (*20*). On analogy with *Ss*EF-1α (*20*, *33*), the GTPase activity of *Ss*(G)EF-1α requires the presence of Mg^{2+} ion (data not shown). These findings suggest that the low affinity of Mg^{2+} for *Ss*EF-1α·GDP is an intrinsic feature of the guanine nucleotide binding domain and does not depend on the interdomain contacts present in the protein. This also indicates that the different behavior of EF-Tu and EF-1α cannot be ascribed to the

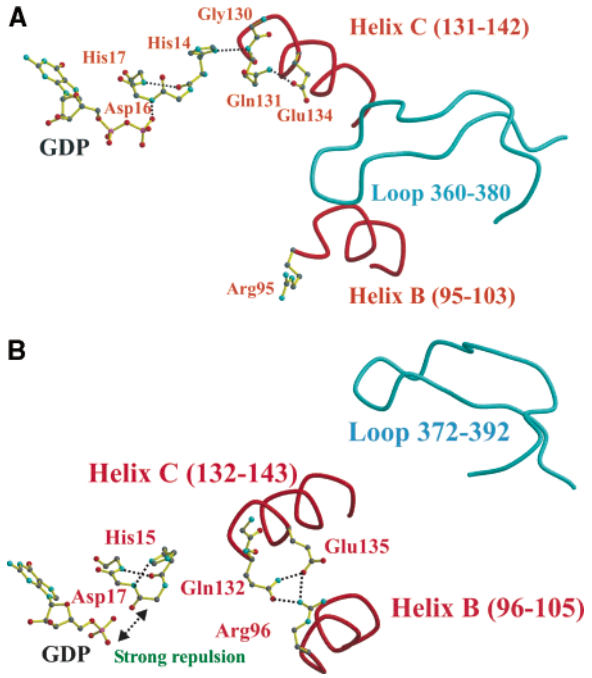

FIGURE 5: Structural modifications induced by the binding of the exchange factor 1β on domain I/domain III interface and on the P-loop region. In panels A and B are reported the structures of *Ss*EF-1α·GDP/Mg^{2+} and *Sc*EF-1β/EF-1α·GDP (*21*), respectively. For clarity, the side chains of residues 15−17 and residues 16−18 have been omitted from panels A and B, respectively. The GDP β-phosphate moiety of *Sc*EF-1β/EF-1α·GDP structure is disordered (*21*).

different relative orientation of helix B and domain III in these two protein systems. It can be surmised that the different role Mg^{2+} plays in EF-Tu and EF-1α may be due to the large sequence (Figure 4) and structure differences occurring in the switch I region, which embodies Asp60 (Asp50 in *E. coli* EF-Tu), a residue potentially involved in the binding of the water molecules coordinating the ion.

Comparison of the Structures of SsEF-1α·GDP/Mg^{2+}, SsEF-1α·GDP, ScEF-1β/EF-1α·GDP, and ScEF-1β/EF-1α: A Detailed Mechanism for the Nucleotide Exchange. The availability of several EF-1α structures (*Ss*EF-1α·GDP/Mg^{2+}, *Ss*EF-1α·GDP, *Sc*EF-1β/EF-1α·GDP, and *Sc*EF-1β/EF-1α) (*19*−*21*), in various binding states, allows the tracing of a detailed structural mechanism of the GDP exchange process.

The relative orientation of the nucleotide binding domain with respect to domains 2 and 3 in *Ss*EF-1α·GDP and *Ss*EF-1α·GDP/Mg^{2+} is completely different to that observed in *Sc*EF-1β/ScEF-1α·GDP (Figure 5). Indeed, the binding of the exchange factor *Sc*EF-1β produces a large rearrangement in *Sc*EF-1α structure (*20*). A rotation of as much as 70° is required to superimpose domains 1 after the superimposition of domains 2 and 3 of *Ss*EF-1α·GDP/Mg^{2+} and *Sc*EF-1β/EF-1α·GDP.

In addition to these overall rearrangements, the binding of EF-1β also produces local alterations that favor the exchange process (Figure 5). In *Ss*EF-1α·GDP/Mg^{2+} (and *Ss*EF-1α·GDP) the helix B is tightly bound to domain 3. Helix B is also rather distant from helix C, which interacts with the P-loop (residues 14−19), through the hydrogen bond Gln131 N atom−His14 $N^{\delta 1}$ atom (*Ss*EF-1α sequence numbering) (Figure 5A). These residues are involved in a rather different interaction pattern in *Sc*EF-1β/EF-1α·GDP (and *Sc*EF-1α/EF-1β). Indeed, due to the overall structural rearrangement associated to the binding of EF-1β, the helix B is no longer involved in strong interactions with domain 3. As a consequence, this helix can establish strong interactions with helix C through the residues Glu135, Gln132, and Arg96 (*Sc*EF-1α sequence numbering) (Figure 5B). The distance between the center of mass of the two helices decreases from 13.7 Å (in *Ss*EF-1α·GDP/Mg^{2+}) to 10.4 Å (in *Sc*EF-1β/EF-1α·GDP). The strong interactions between helix C and helix B weaken the interaction of the former with the P-loop. Indeed, the hydrogen bond between N Gln131 and $N^{\delta 1}$ His14, observed in *Ss*EF-1α·GDP/Mg^{2+}, is lost in *Sc*EF-1β/EF-1α·GDP (and *Sc*EF-1α/EF-1β). As a result, His15 side chain in *Sc*EF-1β/EF-1α·GDP can interact with the N of Asp17, thus favoring the flip of the peptide bond 16−17. The flip destabilizes the interaction of the P-loop with the β-phosphate of the GDP, which becomes disordered in the *Sc*EF-1β/EF-1α·GDP structure (Figure 5B).

It is worth mentioning that all the residues involved in the interactions described above are very well conserved in the sequences of archaea and eukarya EF-1αs. Therefore, the mechanism may be of general validity among EF-1αs.

CONCLUSIONS

The present structural data demonstrate that *Ss*EF-1α·GDP can bind Mg^{2+} at least at nonphysiological concentrations. The analysis of the binding mode of the ion unveils the structural bases for the marginal role that Mg^{2+} plays in the nucleotide exchange process of EF-1α. Indeed, four of the six ligands of the octahedral coordination of the Mg^{2+} are water molecules, which are not involved in interactions with protein residues. A survey of complexes of GTPases with GDP and Mg^{2+} reveals that at least one water molecule of Mg^{2+} coordination is also linked, through hydrogen bonds, to protein atoms. In *Ss*EF-1α·GDP/Mg^{2+} Asp60 and Asp90, which play a role in the binding of the magnesium ion in EF-Tu, are very far from the nucleotide binding site.

The progressive accumulation of structural information on EF-1α highlights the differences between translation elongation factors isolated from bacteria and archaea/eukarya. Paradoxically, Mg^{2+} is essential for GTPase activity (*20*) but not important for nucleotide binding of EF-1α, while the reverse has been reported for *Thermus thermophilus* EF-Tu (*34*). The structure reported here, which likely represents a transient state with the Mg^{2+} still bound to the GDP after the GTP hydrolysis, indicates that the role Mg^{2+} plays in EF-1α is closer to more distant GBNP, such as the heterotrimeric G-protein (*35*), and the small GNBP ARL (*36*), and RhoA (*37*), than to EF-Tu.

ACKNOWLEDGMENT

The authors thank Dr. Giuseppe Perretta for discussion, Mrs Giosue' Sorrentino and Maurizio Amendola for their skilful technical assistance, and Luca De Luca for his help in the photograph layouts. The authors acknowledge ESRF for providing the synchrotron radiation facilities and thank the beamline ID14-1 staff, in particular Dr. Cecile Janin, for the assistance during data collection.

REFERENCES

1. Kjeldgaard, M., Nyborg, J., and Clark, B. F. (1996) The GTP binding motif: variations on a theme. *FASEB J. 10*, 1347−1368.

2. Vetter, I. R., and Wittinghofer, A. (2001) The guanine nucleotide-binding switch in three dimensions. *Science 294*, 1299−1304.
3. Abel, K., and Jurnak, F. (1996) A complex profile of protein elongation: translating chemical energy into molecular movement. *Structure 4*, 229−238.
4. Krab, I. M., and Parmeggiani, A. (2002) Mechanisms of EF-Tu, a pioneer GTPase. *Prog. Nucleic Acid. Res. Mol. Biol. 71*, 513−551.
5. Andersen, G. R., Nissen, P., and Nyborg, J. (2003) Elongation factors in protein biosynthesis. *Trends Biochem. Sci. 28*, 434−441.
6. Kjeldgaard, M., and Nyborg, J. (1992) Refined structure of elongation factor EF-Tu from *Escherichia coli*. *J. Mol. Biol. 223*, 721−742.
7. Andersen, G. R., Thirup, S., Spremulli, L. L., and Nyborg, J. (2000) High-resolution crystal structure of bovine mitochondrial EF-Tu in complex with GDP. *J. Mol. Biol. 297*, 421−436.
8. Abel, K., Yoder, M. D., Hilgenfeld, R., and Jurnak, F. (1996) An alpha to beta conformational switch in EF-Tu. *Structure 4*, 1153−1159.
9. Polekhina, G., Thirup, S., Kjeldgaard, M., Nissen, P., Lippmann, C., and Nyborg, J. (1996) Helix unwinding in the effector region of elongation factor EF-Tu-GDP. *Structure 4*, 1141−1151.
10. Berchtold, H., Reshetnikova, L., Reiser, C. O., Schirmer, N. K., Sprinzl, M., and Hilgenfeld, R. (1993) Crystal structure of active elongation factor Tu reveals major domain rearrangements. *Nature 365*, 126−132.
11. Kjeldgaard, M., Nissen, P., Thirup, S., and Nyborg, J. (1993) The crystal structure of elongation factor EF-Tu from *Thermus aquaticus* in the GTP conformation. *Structure 1*, 35−50.
12. Nissen, P., Kjeldgaard, M., Thirup, S., Polekhina, G., Reshetnikova, L., Clark, B. F., and Nyborg, J. (1995) Crystal structure of the ternary complex of Phe-tRNAPhe, EF-Tu, and a GTP analog. *Science 270*, 1464−1472.
13. Bilgin, N., Ehrenberg, M., Ebel, C., Zaccai, G., Sayers, Z., Koch, M. H. J., Svergun, D. I., Barberato, C., Volkov, V., Nissen, P., and Nyborg, J. (1998) Solution structure of the ternary complex between aminoacyl-tRNA, elongation factor Tu, and guanosine triphosphate. *Biochemistry 37*, 8163−8172.
14. Nissen, P., Thirup, S., Kjeldgaard, M., and Nyborg, J. (1999) The crystal structure of Cys-tRNACys-EF-Tu-GDPNP reveals general and specific features in the ternary complex and in tRNA. *Struct. Folding Des. 7*, 143−156.
15. Kawashima, T., Berthet-Colominas, C., Wulff, M., Cusack, S., and Leberman, R. (1996) The structure of the *Escherichia coli* EF-Tu.EF-Ts complex at 2.5 Å resolution. *Nature 379*, 511−518.
16. Wang, Y., Jiang, Y., Meyering-Voss, M., Sprinzl, M., and Sigler, P. B. (1997) Crystal structure of the EF-Tu.EF-Ts complex from Thermus thermophilus. *Nat. Struct. Biol. 4*, 650−656.
17. Heffron, S. E., and Jurnak, F. (2000) Structure of an EF-Tu complex with a thiazolyl peptide antibiotic determined at 2.35 Å resolution: atomic basis for GE2270A inhibition of EF-Tu. *Biochemistry 39*, 37−45.
18. Vogeley, L., Palm, G. J., Mesters, J. R., and Hilgenfeld, R. (2001) Conformational change of elongation factor Tu (EF-Tu) induced by antibiotic binding. Crystal structure of the complex between EF-Tu•GDP and aurodox. *J. Biol. Chem. 276*, 17149−17155.
19. Andersen, G. R., Pedersen, L., Valente, L., Chatterjee, I., Kinzy, T. G., Kjeldgaard, M., and Nyborg, J. (2000) Structural basis for nucleotide exchange and competition with tRNA in the yeast elongation factor complex eEF1A:eEF1Balpha. *Mol. Cell 6*, 1261−1266.
20. Vitagliano, L., Masullo, M., Sica, F., Zagari, A., and Bocchini, V. (2001) The crystal structure of *Sulfolobus solfataricus* elongation factor 1α in complex with GDP reveals novel features in nucleotide binding and exchange. *EMBO J. 20*, 5305−5311.
21. Andersen, G. R., Valente, L., Pedersen, L., Kinzy, T. G., and Nyborg, J. (2001) Crystal structures of nucleotide exchange intermediates in the eEF1A-eEF1Balpha complex. *Nat. Struct. Biol. 8*, 531−534.
22. Ianniciello, G., Masullo, M., Gallo, M., Arcari, P., and Bocchini, V. (1996) Expression in *Escherichia coli* of thermostable elongation factor 1 alpha from the archaeon *Sulfolobus solfataricus*. *Biotechnol. Appl. Biochem. 23*, 41−45.
23. Zagari, A., Sica, F., Scarano, G., Vitagliano, L., and Bocchini, V. (1994) Crystallization of a hyperthermophilic archaeal elongation factor 1 alpha. *J. Mol. Biol. 242*, 175−177.
24. Otwinowski, Z., and Minor, W. (1997) Processing of X-ray diffraction data collected in oscillation mode. *Methods Enzymol. 276*, 307−326.
25. Jones, T. A., Zou, J. Y., Cowan, S. W., and Kjeldgaard, M. (1991) Improved methods for binding protein models in electron density maps and the location of errors in these models. *Acta Crystallogr., Sect. A: Found. Crystallogr. 47*, 110−119.
26. Kraulis, P. J. (1991) MOLSCRIPT: A program to produce both detailed and schematic plots of protein structures. *J. Appl. Crystallogr. 24*, 946−950.
27. Esnouf, R. M. (1999) Further additions to MolScript version 1.4, including reading and conturing of electron-density maps. *Acta Crystallogr., Sect. D: Biol. Crystallogr. 55*, 938−940.
28. Merritt, E. A., and Bacon, D. J. (1997) Raster3D: photorealistic molecular graphics. *Methods Enzymol. 277*, 505−524.
29. Masullo, M., Ianniciello, G., Arcari, P., and Bocchini, V. (1997) Properties of truncated forms of the elongation factor 1alpha from the archaeon *Sulfolobus solfataricus*. *Eur. J. Biochem. 243*, 468−473.
30. Buglino, J., Shen, V., Hakimian, P., and Lima, C. D. (2002) Structural and biochemical analysis of the Obg GTP binding protein. *Structure 10*, 1581−1592.
31. Nystrom, T. (2003) Conditional senescence in bacteria: death of the immortals. *Mol. Microbiol. 48*, 17−23.
32. Song, H., Parsons, M. R., Rowsell, S., Leonard, G., and Phillips, S. E. (1999) Crystal structure of intact elongation factor EF-Tu from *Escherichia coli* in GDP conformation at 2.05 Å resolution. *J. Mol. Biol. 285*, 1245−1256.
33. Masullo, M., De Vendittis, E., and Bocchini, V. (1994) Archaebacterial elongation factor 1 alpha carries the catalytic site for GTP hydrolysis. *J. Biol. Chem. 269*, 20376−20379.
34. Rutthard, H., Banerjee, A., and Makinen, M. W. (2001) Mg^{2+} Is Not Catalytically Required in the Intrinsic and Kirromycin-stimulated GTPase Action of Thermus thermophilus EF-Tu. *J. Biol. Chem. 276*, 18728−18733.
35. Coleman, D. E., and Sprang, S. R. (1998) Crystal structures of the G protein Gi alpha 1 complexed with GDP and Mg^{2+}: A crystallographic titration experiment. *Biochemistry 37*, 14376−14385.
36. Hillig, R. C., Hanzal-Bayer, M., Linari, M., Becker, J., Wittinghofer, A., and Renault, L. (2000) Structural and biochemical properties show ARL3-GDP as a distinct GTP binding protein. *Struct. Folding Des. 8*, 1239−1245.
37. Shimizu, T., Ihara, K., Maesaki, R., Kuroda, S., Kaibuchi, K., and Hakoshima, T. (2000) An open conformation of switch I revealed by the crystal structure of a Mg^{2+}-free form of RHOA complexed with GDP. Implications for the GDP/GTP exchange mechanism. *J. Biol. Chem. 275*, 18311−18317.

BI0363331